Scattering at Circular-to-Rectangular Waveguide Junctions

JOHN DOUGLAS WADE AND ROBERT H. MACPHIE, SENIOR MEMBER, IEEE

Abstract—**A formally exact solution is given for the problem of scattering at a circular-to-rectangular waveguide junction and at a thick diaphragm, with a centered circular aperture, in a rectangular waveguide. The method uses normal TE and TM mode expansions of the waveguide fields and traditional mode matching of the transverse electric and magnetic fields at the junction boundary. Exact closed-form expressions are obtained for the electric field mode-matching coefficients which couple the TE(TM) modes in the rectangular guide to the TE(TM) and TM(TE) modes in the circular guide. Numerical results are presented for the case of TE_{10} mode propagation in the larger rectangular guide with all other modes cutoff. Convergent numerical results for the equivalent shunt susceptances of such junctions are obtained when about 12 modes (eight TE and four TM) are retained in the circular waveguide or in the circular aperture of the diaphragm. The results are graphically compared with formulas and curves due to the quasi-static theory of Bethe and the variational theory given in the *Waveguide Handbook* [2].**

I. Introduction

ELECTROMAGNETIC DIFFRACTION by a circular aperture in a conducting screen is important in microwave engineering. Waveguide diaphragms with circular apertures can be used as matching elements in microwave circuits or in the construction of cavity filters. Waveguide-to-cavity coupling is often accomplished with a circular aperture.

The theory of diffraction by small holes was pioneered by Bethe [1]. He showed that a small aperture in a conducting screen is approximately equivalent to an electric dipole normal to the screen with a strength proportional to the normal component of the exciting field, and a magnetic dipole in the plane of the screen with a strength proportional to the exciting tangential magnetic field.

The most complete variational solution of scattering from a diaphragm with centered circular aperture in a rectangular waveguide is given in Marcuvitz [2, pp. 238–240]. The equivalent circuit for the aperture consists of a susceptance shunted between two wires of a transmission line. Full mode expansions of the waveguide fields are used but the aperture E field is approximated with a static, small-hole distribution. Therefore, these formulas will be less accurate for larger holes.

Manuscript received January 28, 1986; revised June 27, 1986. This work was supported in part by the Natural Science and Engineering Research Council, Ottawa, Canada, under Grant A-2176.

J. D. Wade is with the National Research Council's Herzberg Institute for Astrophysics in Ottawa, Canada K1A OR6.

R. H. MacPhie is with the Electrical Engineering Department, University of Waterloo, Waterloo, Ontario, Canada N2L 3G1.

IEEE Log Number 8610510.

Modal analysis, coupled with the technique of matching the tangential electric and magnetic fields at waveguide junction discontinuities, has been used to solve a variety of problems [3]–[6]. Modal analysis suffers from the relative convergence problem, but this can be eliminated by a judicious choice for the ratio of the number of modes used for the aperture field expansion to the number of modes used for the waveguide field expansion [7], [8].

In this paper, modal analysis and the matching of the E and H fields at the junction of a circular and a rectangular waveguide lead to a closed-form analytical solution for the scattering matrix $[S]$ of the junction. It is demonstrated that convergent numerical results for the dominant-mode (TE_{11} or TE_{10}) reflection and transmission coefficients can be obtained by retaining about 12 modes (eight TE and four TM) in the smaller, circular waveguide (see Fig. 1). The case of a thick diaphragm, with a centered circular hole, in a rectangular waveguide is then treated as a cascaded connection of rectangular–circular–rectangular guides. The generalized scattering matrix technique [8], [9] is used to deduce the scattering matrix $[S^d]$ of the diaphragm. In both cases (simple circular-to-rectangular junction and the rectangular–circular–rectangular diaphragm junction), the numerical results are presented in terms of the inductive shunting susceptances across equivalent transmission lines. The results are compared with the formulas and curves due to Bethe [1], [10] and those in the *Waveguide Handbook*.

II. Electric Field Mode Matching at the Junction

As illustrated in Fig. 1, the circular waveguide of radius R (guide 1) forms a junction at $z = 0$ with a larger rectangular waveguide of lateral dimensions a and b (guide 2), with $b \geqslant 2R$. Note that the z axis is the axis of symmetry for *both* guides. The more general problem of a junction with laterally displaced axes appears to have a solution based on the techniques given in this paper but, at present, the details have not been worked out.

In the circular waveguide (guide 1 for which $z < 0$), the tangential electric field just to the left of the junction ($z = 0$) can be given as a superposition of TE (h-type) and TM (e-type) modal fields:

$$\vec{e}_1(\rho,\phi) = \sum_q \sum_r \left[a_{qr}^{(h)} \vec{e}_{1,qr}^{(h)}(\rho,\phi) + a_{qr}^{(e)} \vec{e}_{1,qr}^{(e)}(\rho,\phi) \right]. \quad (1)$$

0018-9480/86/1100-1085$01.00 ©1986 IEEE

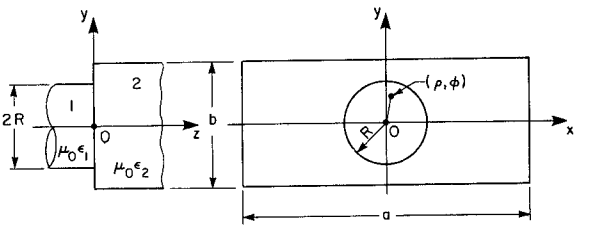

Fig. 1. A circular-to-rectangular waveguide junction. Guides have a common axis of symmetry (z axis).

Traditionally, the modal fields in (1) are written as (see Collin [10, p. 110])

$$\vec{e}_{1,qr}^{(h)}(\rho,\phi) = N_{qr}^{(h)}\left[\hat{\rho}(q/\rho)J_q(\beta'_{qr}\rho)\cdot\sin(q\phi) + \hat{\phi}\beta'_{qr}J'_q(\beta'_{qr}\rho)\cos(q\phi)\right] \quad (2)$$

$$\vec{e}_{1,qr}^{(e)}(\rho,\phi) = N_{qr}^{(e)}\left[\hat{\rho}\beta''_{qr}J'_{qr}(\beta''_{qr}\rho)\cdot\sin(q\phi) + \hat{\phi}(q/\rho)J_q(\beta''_{qr}\rho)\cos(q\phi)\right] \quad (3)$$

where

$$N_{qr}^{(h)} = \frac{\sqrt{\frac{2}{\pi}}}{\sqrt{(\beta'_{qr}R)^2 - q^2J_q^2(\beta'_{qr}R)}}$$

and

$$N_{qr}^{(e)} = \frac{\sqrt{\frac{\pi}{2}}}{\beta''_{qr}RJ'_q(\beta''_{qr}R)}$$

are normalization constants in which $\beta'_{qr}R$ and $\beta''_{qr}R$ are, respectively, the rth roots of $J'_q(x)$ and $J_q(x)$.

However, for the circular-to-rectangular junction, it is convenient to replace the *unit vectors* $\hat{\rho}$ and $\hat{\phi}$ in (2) and (3) by their *Cartesian* $(\hat{x}, \hat{y})$ *equivalents*. It is not difficult to show that (2) and (3) can be reexpressed as follows:

$$\vec{e}_{1,qr}^{(h)}(\rho,\phi) = \frac{\beta'_{qr}N_{qr}^{(h)}}{2}\left[J_{q-1}(\beta'_{qr}\rho)\hat{E}_{q-1}(\phi) + J_{q+1}(\beta'_{qr}\rho)\hat{E}_{q+1}(\phi)\right] \quad (4)$$

$$\vec{e}_{1,qr}^{(e)}(\rho,\phi) = \frac{\beta''_{qr}N_{qr}^{(e)}}{2}\left[J_{q-1}(\beta''_{qr}\rho)\hat{E}_{q-1}(\phi) - J_{q+1}(\beta''_{qr}\rho)\hat{E}_{q+1}(\phi)\right] \quad (5)$$

where

$$\hat{E}_{q\pm1}(\phi) = \hat{x}\sin[(q\pm1)\phi] \mp \hat{y}\cos[(q\pm1)\phi] \quad (6)$$

are ϕ-dependent unit vectors.

In the rectangular waveguide (guide 2 for which $z > 0$), with the z axis passing along its center and not along its lower left corner (as is normally assumed), the modes for which the E fields are *even functions* of both x and y would be those scattered by a TE_{10} mode field incident from guide 2 or a TE_{11} mode incident from guide 1. In this case of greatest practical interest, the tangential E field just to the right of the junction ($z = 0+$) can be expanded as follows:

$$\vec{e}_2(x,y) = \sum_m\sum_n\left[b_{mn}^{(h)}\vec{e}_{2,mn}^{(h)}(x,y) + b_{mn}^{(e)}\vec{e}_{2,mn}^{(e)}(x,y)\right] \quad (7)$$

with $m = 1,3,5,\cdots$ and $n = 0,2,4,\cdots$.

Moreover, to obtain E fields with even symmetry with respect to the x and y axes in the circular waveguide, the series expansion (1) is for *odd* q ($q = 1,3,5,\cdots$).

In (7), the modal fields are

$$\vec{e}_{2,mn}^{(h)}(x,y) = N_{mn}\left[\hat{x}\beta_{yn}\sin(\beta_{xm}x)\sin(\beta_{yn}y) + \hat{y}\beta_{xm}\cos(\beta_{xm}x)\cos(\beta_{yn}y)\right] \quad (8)$$

$$\vec{e}_{2,mn}^{(e)}(x,y) = N_{mn}\left[\hat{x}\beta_{xm}\sin(\beta_{xm}x)\sin(\beta_{yn}y) - \hat{y}\beta_{yn}\cos(\beta_{xm}x)\cos(\beta_{yn}y)\right] \quad (9)$$

where

$$N_{mn} = 2\Big/\sqrt{ab\left[\beta_{yn}^2 + 2\beta_{xm}^2/\epsilon_n\right]} \quad (10)$$

is the rectangular waveguide modal normalization factor, in which

$$\beta_{xm}a = m\pi,\ \beta_{yn}b = n\pi \text{ and } \epsilon_n = 1 \text{ if } n = 0,\ \epsilon_n = 2 \text{ if } n \neq 0.$$

However, we now find it convenient in this circular-to-rectangular waveguide junction problem to transform the *coordinates* (x, y) in (8) and (9) into their *circular cylindrical equivalents*. First, one can show that the double sine product occurring in (8) and (9) can be written as

$$\sin(\beta_{xm}x)\sin(\beta_{yn}y) = \sin[\beta_{mn}\cos\phi_{mn}\rho\cos\phi]\sin[\beta_{mn}\sin\phi_{mn}\rho\sin\phi]$$

where

$$\rho^2 = x^2 + y^2 \qquad \beta_{mn}^2 = \beta_{xm}^2 + \beta_{yn}^2,$$

$$\phi = \tan^{-1}\left(\frac{y}{x}\right) \text{ and } \phi_{mn} = \tan^{-1}\left(\frac{\beta_{yn}}{\beta_{xm}}\right).$$

Then, by means of standard trigonometric identities and a well-known Bessel–Fourier expansion [11, p. 361], we find that

$$\sin(\beta_{xm}x)\sin(\beta_{yn}y) = -\sum_{p=1}^{\infty}(-1)^pJ_{2p}(\beta_{mn}\rho)\sin(2p\phi_{mn})\sin(2p\phi). \quad (11)$$

Moreover, in the same way, one can verify that

$$\cos(\beta_{xm}x)\cos(\beta_{yn}y) = \sum_{p=0}^{\infty}\epsilon_p(-1)^pJ_{2p}(\beta_{mn}\rho)\cdot\cos(2p\phi_{mn})\cos(2p\phi). \quad (12)$$

Use of (11) and (12) in (8) and (9) leads to

$$\vec{e}_{2,mn}^{(h)}(\rho,\phi) = N_{mn} \sum_{p=0}^{\infty} J_{2p}(\beta_{mn}\rho) \cdot \left[\beta_{yn} S_{mn,p}(\phi)\hat{x} + \beta_{xm} C_{mn,p}(\phi)\hat{y}\right] \quad (13)$$

$$\vec{e}_{2,mn}^{(e)}(\rho,\phi) = N_{mn} \sum_{p=0}^{\infty} J_{2p}(\beta_{mn}\rho) \cdot \left[\beta_{xm} S_{mn,p}(\phi)\hat{x} - \beta_{yn} C_{mn,p}(\phi)\hat{y}\right] \quad (14)$$

wherein

$$S_{mn,p}(\phi) = -(-1)^p \sin(2p\phi_{mn}) \sin(2p\phi) \quad (15)$$

$$C_{mn,p}(\phi) = \epsilon_p (-1)^p \cos(2p\phi_{mn}) \cos(2p\phi). \quad (16)$$

We are now in a position to enforce the electromagnetic boundary conditions on the transverse electric field at the circular-to-rectangular waveguide junction. The field must be continuous (matched) in the circular aperture $0 < \rho < R$ and vanish everywhere else in the region $2|x| < a, 2|y| < b$; we tacitly assume that the conductivity of all the metal surfaces is infinite. Thus, the boundary conditions are such that

$$\vec{e}_2(\rho,\phi) = \begin{cases} \vec{e}_1(\rho,\phi), & 0 < \rho \leqslant R, \\ 0, & \rho > R \text{ and } 2|x| < a, 2|y| < b. \end{cases} \quad (17)$$

Using (1) and (7) in (17) gives

$$\sum_{\bar{m}} \sum_{\bar{n}} b_{\bar{m}\bar{n}}^{(h)} \vec{e}_{2,\bar{m}\bar{n}}^{(h)}(\rho,\phi) + b_{\bar{m}\bar{n}}^{(e)} \vec{e}_{2,\bar{m}\bar{n}}^{(e)}(\rho,\phi) = \begin{cases} \sum_q \sum_r a_{qr}^{(h)} \vec{e}_{1,qr}^{(h)}(\rho,\phi) + a_{qr}^{(e)} \vec{e}_{1,qr}^{(e)}(\rho,\phi), & 0 < \rho \leqslant R \\ 0, \quad \rho > R \text{ and } 2|x| < a, 2|y| < b. \end{cases} \quad (18)$$

Scalar multiplication of (18) by $\vec{e}_{2,mn}^{(h)}(\rho,\phi)$ and integration over the complete cross section of guide 2 yields, due to the orthogonality of the guide 2 modes,

$$b_{mn}^{(h)} = \sum_q \sum_r H_{mn,qr} a_{qr}^{(h)} + K_{mn,qr} a_{qr}^{(e)} \quad (19)$$

where

$$H_{mn,qr} = \int_0^{2\pi} \int_0^R \vec{e}_{2,mn}^{(h)}(\rho,\phi) \cdot \vec{e}_{1,qr}^{(h)}(\rho,\phi) \rho \, d\rho \, d\phi \quad (20)$$

and

$$K_{mn,qr} = \int_0^{2\pi} \int_0^R \vec{e}_{2,mn}^{(h)}(\rho,\phi) \cdot \vec{e}_{1,qr}^{(e)}(\rho,\phi) \rho \, d\rho \, d\phi \quad (21)$$

are, respectively, the TE–TE and TE–TM E-field mode-coupling coefficients for the junction.

These coefficient integrals can be evaluated analytically if we use (4)–(6) and (13), (15), and (16) in (20) and (21). Then, in view of orthogonality of the Fourier harmonics $[\sin(q \pm 1)\phi, \cos(q \pm 1)\phi]$ and a Bessel function integral provided by Abramowitz and Stegun [11, p. 484, eq. (11.3.29)], one can show that

$$H_{mn,qr} = A_{mn,q} N_{mn} N_{qr}^{(h)} \cos(q\phi_{mn}) \cdot \left[B'_{mn,q-1,r} + B'_{mn,q+1,r}\right] \quad (20a)$$

$$K_{mn,qr} = A_{mn,q} N_{mn} N_{qr}^{(e)} \cos(q\phi_{mn}) \cdot \left[B''_{mn,q-1,r} - B''_{mn,q+1,r}\right] \quad (21a)$$

where

$$A_{mn,q} = 2\pi(-1)^{(q-1)/2} \beta_{mn} \quad (22)$$

and

$$B^{\iota}_{mn,q\pm1,r} = \frac{1}{2} \frac{\beta^{\iota}_{qr} R}{\beta_{mn}^2 - \beta_{qr}^{\iota 2}} \left[\beta_{mn} J_{q+2}(\beta_{mn}R) J_{q\pm1}(\beta^{\iota}_{qr}R) - \beta^{\iota}_{qr} J_{q+2}(\beta^{\iota}_{qr}R) J_{q\pm1}(\beta_{mn}R)\right] \quad (23)$$

with $\iota = '$ or $''$.

However, by making use of the fact that $J_q(\beta''_{qr}R) = 0$, we can, with recursion formulas for Bessel functions, show that (21a) *vanishes*, i.e.,

$$K_{mn,qr} = 0. \quad (21b)$$

This curious phenomenon also occurs for the rectangular-to-rectangular waveguide junction [9, p. 2061].

If we now scalar multiply (18) by $\vec{e}_{2,mn}^{(e)}(\rho,\phi)$ and integrate over the rectangular cross section at $z = 0$, we obtain

$$b_{mn}^{(e)} = \sum_q \sum_r Q_{mn,qr} a_{qr}^{(h)} + E_{mn,qr} a_{qr}^{(e)} \quad (24)$$

where

$$Q_{mn,qr} = \int_0^{2\pi} \int_0^R \vec{e}_{2,mn}^{(e)}(\rho,\phi) \cdot \vec{e}_{1,qr}^{(h)}(\rho,\phi) \rho \, d\rho \, d\phi \quad (25)$$

$$E_{mn,qr} = \int_0^{2\pi} \int_0^R \vec{e}_{2,mn}^{(e)}(\rho,\phi) \cdot \vec{e}_{1qr}^{(e)}(\rho,\phi) \rho \, d\rho \, d\phi. \quad (26)$$

Again, closed-form expressions for these coupling coefficients (TM–TE and TM–TM) can be deduced

$$Q_{mn,qr} = -A_{mn,q} N_{mn} N_{qr}^{(h)} \sin(q\phi_{mn}) \cdot \left[B'_{mn,q-1,r} - B'_{mn,q+1,r}\right] \quad (25a)$$

$$E_{mn,qr} = -A_{mn,q} N_{mn} N_{qr}^{(e)} \sin(q\phi_{mn}) \cdot \left[B''_{mn,q-1,r} + B''_{mn,q+1,r}\right]. \quad (26a)$$

The latter can be shown to reduce to

$$E_{mn,qr} = \frac{-\beta_{mn}\beta''_{qr} R A_{mn,q} N_{mn} N_{qr}^{(e)}}{2\left(\beta_{mn}^2 - \beta_{qr}''^2\right)} \cdot \sin(q\phi_{mn}) J_q(\beta_{mn}R) J_{q-1}(\beta''_{qr}R). \quad (26b)$$

Equations (19) and (24) can be cast into matrix form as follows:

$$\begin{bmatrix} \boldsymbol{b}^{(h)} \\ \boldsymbol{b}^{(e)} \end{bmatrix} = \begin{bmatrix} [H] & [0] \\ [Q] & [E] \end{bmatrix} \begin{bmatrix} \boldsymbol{a}^{(h)} \\ \boldsymbol{a}^{(e)} \end{bmatrix} \quad (27)$$

where $\boldsymbol{a}^{(m)}$ and $\boldsymbol{b}^{(m)}$, with $m=h$ or e, being the modal weighting coefficient vectors in guides 1 and 2, respectively, and $[H]$, $[0]=[K]$, $[Q]$ and $[E]$ being the submatrices of the overall E-field mode-matching matrix $[M]$, with

$$\boldsymbol{b}=[M]\boldsymbol{a} \tag{28}$$

and

$$\boldsymbol{a}^T=[\boldsymbol{a}^{(h)T},\boldsymbol{a}^{(e)T}] \qquad \boldsymbol{b}^T=[\boldsymbol{b}^{(h)T},\boldsymbol{b}^{(e)T}]$$

with T indicating the transpose operator.

III. The Scattering Matrix of the Circular–Rectangular Junction

We define the E-field modal coefficient scattering matrix $[S]$ of the circular-to-rectangular waveguide junction to be such that

$$\begin{bmatrix}\boldsymbol{a}^-\\ \boldsymbol{b}^-\end{bmatrix}=\begin{bmatrix}[S_{11}] & [S_{12}]\\ [S_{21}] & [S_{22}]\end{bmatrix}\begin{bmatrix}\boldsymbol{a}^+\\ \boldsymbol{b}^+\end{bmatrix} \tag{29}$$

where, as is traditional, the + and − superscripts denote, respectively, incident and scattered waves.

In the case of the lossless structure, one can use H-field mode matching in the circular junction aperture to deduce the following matrix equation:

$$[M]^T[Y_2](\boldsymbol{b}^- - \boldsymbol{b}^+)=[Y_1](\boldsymbol{a}^+ - \boldsymbol{a}^-). \tag{30}$$

H-field mode matching, analogous to the E-field mode matching described in Section II, is well known [3], [5] and will not be treated in detail in this paper. In (30) $[Y_i]$, for $i=1$ and 2, is the modal admittance matrix for the ith guide.

$$[Y_i]=\begin{bmatrix}[Y_i^{(h)}] & [0]\\ [0] & [Y_i^{(e)}]\end{bmatrix} \tag{31}$$

where the two submatrices in (31) are diagonal. In particular, for the circular guide, the diagonal elements are

$$Y_{1,qr}^{(h)}=\frac{\sqrt{\beta_{qr}'^2-k_1^2}}{j\omega\mu_0} \qquad Y_{1qr}^{(e)}=\frac{j\omega\epsilon_1}{\sqrt{\beta_{qr}''^2-k_1^2}} \tag{32}$$

and for the rectangular guide they are

$$Y_{2,mn}^{(h)}=\frac{\sqrt{\left(\frac{m\pi}{a}\right)^2+\left(\frac{n\pi}{b}\right)^2-k_2^2}}{j\omega\mu_0}$$

$$Y_{2mn}^{(e)}=\frac{j\omega\epsilon_2}{\sqrt{\left(\frac{m\pi}{a}\right)^2+\left(\frac{n\pi}{b}\right)^2-k_2^2}}. \tag{33}$$

In (32) and (33), μ_0 is the permeability and ϵ_1 and ϵ_2 are the permittivities of the dielectrics filling guides 1 and 2, respectively.

Then, if we assume that incidence is from guide 1 only, so that $\boldsymbol{b}^+=0$, it is straightforward to show, using (28) and (30), that

$$\boldsymbol{a}^-=\left\{([Y_1]+[Y_{L1}])^{-1}([Y_1]-[Y_{L1}])\right\}\boldsymbol{a}_+ \tag{34}$$

where

$$[Y_{L1}]=[M]^T[Y_2][M] \tag{35}$$

is the "load" admittance matrix of guide 2 as "seen" by guide 1. In view of the fact that $\boldsymbol{b}^+=0$, it follows from (29) that

$$[S_{11}]=([Y_1]+[Y_{L1}])^{-1}([Y_1]-[Y_{L1}]). \tag{36}$$

The other submatrices in (29) are then deduced by simple matrix algebra

$$[S_{21}]=[M]([S_{11}]+[I]) \tag{37}$$

$$[S_{12}]=2([Y_1]+[Y_{L1}])^{-1}[M]^T[Y_2] \tag{38}$$

$$[S_{22}]=[M][S_{12}]-[I] \tag{39}$$

where $[I]$ is the identity matrix and T indicates the transpose operation. These results may also be obtained by means of the conservation of complex power technique [9], [12].

IV. Transverse Diaphragm with Centered Circular Hole in Rectangular Waveguide

Fig. 2 illustrates the geometry of a diaphragm (perfectly conducting) of nonzero thickness l with a centered circular hole of radius R. This structure can be regarded as a rectangular–circular–rectangular cascaded connection and the generalized scattering matrix technique [8, pp. 207–217] may be used to determine the overall scattering matrix $[S^d]$ of the diaphragm

$$[S_{11}^d]=[S_{33}^d]=[S_{11}]+[S_{12}][L][S_{22}]$$
$$\cdot\{[I]-[L][S_{22}][L][S_{22}][L][S_{22}]\}^{-1}[L][S_{21}] \tag{40}$$

$$[S_{13}^d]=[S_{31}^d]$$
$$=[S_{12}]\{[I-[L][S_{22}][L][S_{22}]\}^{-1}[L][S_{21}]. \tag{41}$$

Here, the transmission-line matrix $[L]$ of the central circular guide is a diagonal matrix such that

$$[L]=\begin{bmatrix}[L^{(h)}] & [0]\\ [0] & [L^{(e)}]\end{bmatrix} \tag{42}$$

with submatrix diagonal elements given by

$$L_{qr,qr}^{(h)}=\exp\left(-\sqrt{\beta_{2,qr}'^2-k_2^2}\,l\right)$$

$$L_{qr,qr}^{(e)}=\exp\left(-\sqrt{\beta_{2,qr}''^2-k_2^2}\,l\right). \tag{43}$$

In (43), the subscript 2 denotes the circular guide (see Fig. 2).

V. Numerical Results

We begin with the case of a circular–rectangular waveguide junction. In our numerical computations, which consider only air-filled guides, we selected a frequency range

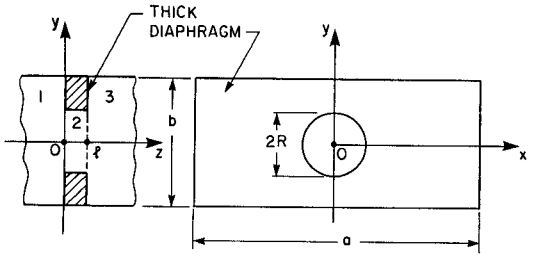

Fig. 2. A thick diaphragm, with centered circular hole, in a rectangular waveguide.

for which the only propagating mode in the larger rectangular guide was the TE_{10} mode. Consequently, there were no propagating modes in the smaller circular guide. Thus, the reflection coefficient ρ_{10} of the TE_{10} mode in the rectangular guide was of primary interest

$$\rho_{10} = S_{22,10,10}. \tag{44}$$

From ρ_{10} one can determine the normalized load admittance (for TE_{10} rectangular modes) of the junction

$$\overline{Y}_J = -j\overline{B}_J = \frac{1-\rho_{10}}{1+\rho_{10}} \tag{45}$$

which is pure imaginary since the circular guide is cut off. Moreover, the minus sign indicates that the junction susceptance is *inductive*.

In the numerical work, the number of modes assumed in each waveguide strongly depends on the size of the circular guide relative to the rectangular. Table I provides the relevant information. Normally, half as many TM modes as TE modes are used in the circular guide. Moreover, as R/b diminishes and with $a = (9/4)b$, the number of rectangular guide modes increases dramatically. Fortunately, this large number of modes need only be used in the calculation of the load admittance matrix $[Y_{L1}]$ as given by (35); therefore *no inversion* of a large matrix is required. Tables II and III show the convergence of $\overline{B}_J$ together with $\overline{B}_D$ for the thin diaphragm with a circular hole as a function of the number of modes in the circular guide for various values of R/b and at two frequencies; the rectangular guide is assumed to be standard X-band guide with $a = 2.286$ cm. It is seen in Tables II and III that for about a dozen modes (eight TE and four TM) in the circular guide, the numerical results have converged quite well for all R/b ratios and at both the low and high frequencies.

In Fig. 3, the susceptance B_J is plotted as a function of a/λ with R/b as a parameter. Twelve modes were used in the circular guide in all cases. Not surprisingly, the normalized susceptance increases as the circular waveguide radius decreases and diverges as $a/\lambda \to 0.5$, since the rectangular TE_{10} mode's admittance vanishes at this point.

Also plotted at discrete values of a/λ are the load susceptances given in the *Waveguide Handbook* [2, p. 327]. For small irises, one has

$$\overline{B}_J = \frac{0.446ab\lambda_g}{D^3}\sqrt{1-\left(\frac{1.706D}{\lambda_g}\right)^2} - \frac{\overline{B}_D}{2} \tag{46}$$

TABLE I
NUMBER OF RECTANGULAR MODES FOR A GIVEN NUMBER OF CIRCULAR MODES

Number of Circular Modes (TE,TM)	Number of Rectangular Modes (TE,TM)			
	R=b/2	R=3b/8	R=b/4	R=b/8
2,1	13,6	20,10	40,25	155,95
4,2	18,10	35,20	65,50	275,20
8,4	35,20	65,40	130,90	500,350

TABLE II
CONVERGENCE OF $\overline{B}_J$ AND $\overline{B}_D$ AT 8 GHz

R	b/2		3b/8		b/4		b/8	
Num. of Modes TE, TM	$\overline{B}_J$	$\overline{B}_D$	$\overline{B}_J$	$\overline{B}_D$	$\overline{B}_J$	$\overline{B}_D$	$\overline{B}_J$	$\overline{B}_D$
2,1	9.62	6.85	23.7	17.4	82.1	61.8	670	514
4,2	9.18	6.15	22.6	15.7	78.0	55.7	632	466
8,4	9.11	6.01	22.4	15.4	77.2	54.6	628	454

$a = 2.25b = 2.286$ cm.

TABLE III
CONVERGENCE OF $\overline{B}_J$ AND $\overline{B}_D$ AT 14 GHz

R	b/2		3b/8		b/4		b/8	
Num. of Modes TE, TM	$\overline{B}_J$	$\overline{B}_D$	$\overline{B}_J$	$\overline{B}_D$	$\overline{B}_J$	$\overline{B}_D$	$\overline{B}_J$	$\overline{B}_D$
2,1	2.56	2.08	7.39	5.41	28.0	20.4	242	184
4,2	2.45	1.87	7.04	4.83	26.6	18.2	230	166
8,4	2.44	1.86	6.99	4.76	26.3	17.9	227	162

$a = 2.25b = 2.286$ cm.

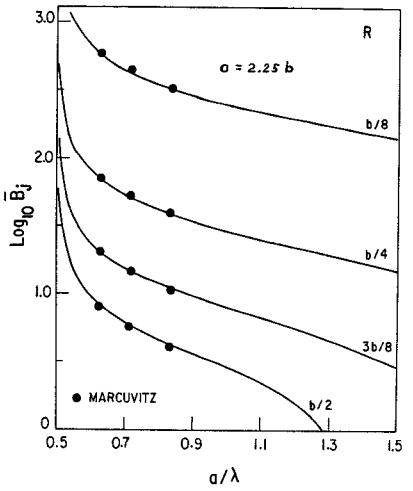

Fig. 3. Susceptance of rectangular-to-circular waveguide junction.

where $D = 2R$ and λ_g is the wavelength of the propagating mode in the rectangular waveguide. The values for $\overline{B}_D$ can be obtained from a graph elsewhere in the handbook [2, p. 240]. We note that the agreement between the quasi-static variational solution (46) and the more rigorous scattering matrix solution (solid lines in Fig. 3) is quite good, even for large values of R/b.

Numerical results for the more interesting case of a thin ($l = 0$) diaphragm with centered circular aperture in a rectangular guide are presented in Fig. 4. Again, it is convenient to represent the zero-thickness diaphragm as a shunting susceptance $\overline{B}_D = B_D/Y_{10}$ normalized with re-

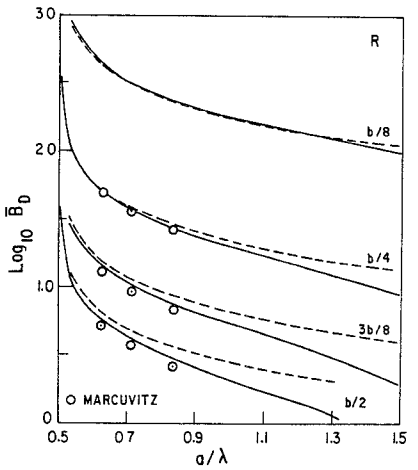

Fig. 4. Susceptance of a thin diaphragm with circular aperture. Solid lines are calculated using the present method while broken lines are from the small-hole formula.

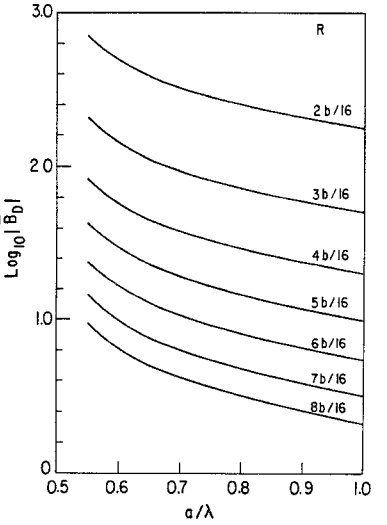

Fig. 5. Susceptance of a thin diaphragm, with a centered circular aperture of radius R, in a rectangular waveguide ($a = 2.25b$).

spect to the rectangular TE_{10} mode's admittance. $\bar{B}_D$ is computed for four aperture radii, and the convergence behavior is indicated in Tables II and III. For twelve modes in the circular guide, it is estimated that the error in $\bar{B}_D$ is 2 percent or less. Also given in Fig. 4 are curves based on the well-established formula

$$\bar{B}_D = \frac{3ab\lambda_g}{16\pi R^3}, \qquad R \ll \lambda_g \tag{47}$$

derived in Collin [10, pp. 190–194] and originating with the quasi-static theory of Bethe [1]. As expected, (47) agrees well with the present results for small holes, $R \leqslant b/8$. For larger apertures, the simple formula overestimates $\bar{B}_D$ and hence underestimates the transmitted field. Bethe shows that for small apertures the fields scattered in the forward direction are proportional to R^3/λ^2, whereas for large Kirchhoff-type apertures they vary as R^2/λ. Accordingly, as R/λ increases (but in our case still remains less than unity), the small-aperture (Bethe) theory predicts a forward scattered field that is too weak and hence a $\bar{B}_D$ that is too large. This is confirmed by the results presented in Fig. 4.

The diaphragm's susceptance is also compared with the variational calculus susceptance provided by the *Waveguide Handbook* [2, p. 240]. The latter gives lower susceptances than the small-hole expression, but for large holes ($R = b/2$) gives values that differ from ours by about 10 percent.

Fig. 5 provides curves of $\bar{B}_D$ for seven different ratios of R/b. The range of a/λ is only over that in which the TE_{10} mode alone can propagate, i.e., the range of greatest practical interest.

We next turn to the case of a diaphragm of nonzero thickness ($l \neq 0$). When the normalized load admittance is calculated, the real part is no longer unity. A more sophisticated circuit representation is thus required. We have chosen the π-equivalent circuit shown in Fig. 6. It

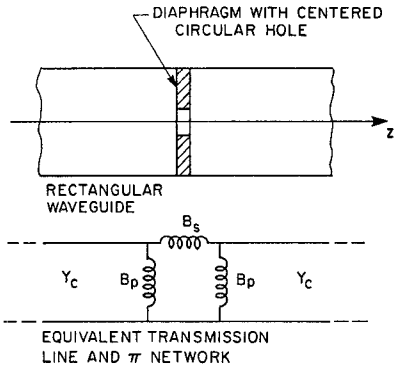

Fig. 6. Thick diaphragm with centered circular hole in rectangular waveguide and the equivalent transmission line with Π network.

can be shown that

$$j\bar{B}_p = \frac{(1-\tau_{10})^2 - \rho_{10}^2}{(1+\rho_{10})^2 - \tau_{10}^2} \tag{48}$$

$$j\bar{B}_S = \frac{2\tau_{10}}{(1+\rho_{10})^2 - \tau_{10}^2} \tag{49}$$

where

$$\tau_{10} = S_{31,10,10} \tag{50}$$

is the transmission coefficient of the TE_{10} mode and is such that

$$|\rho_{10}|^2 + |\tau_{10}|^2 = 1 \tag{51a}$$

$$\arg(\rho_{10}) - \arg(\tau_{10}) = \pi/2. \tag{51b}$$

Clearly $\bar{B}_P$ and $\bar{B}_S$ can be deduced from a knowledge of τ_{10} alone. We choose $|\tau_{10}|$ and $\arg(\tau_{10})$ for our graphical results since $\bar{B}_S \to \infty$ when $l \to 0$. The amplitude of τ_{10} is plotted in Fig. 7(a) for four aperture radii and a series of diaphragm thicknesses ranging in increments of $\Delta l/a = 0.02$ from $l/a = 0$ to $l/a = 0.08$. As is expected, the transmitted wave's amplitude decreases with increasing di-

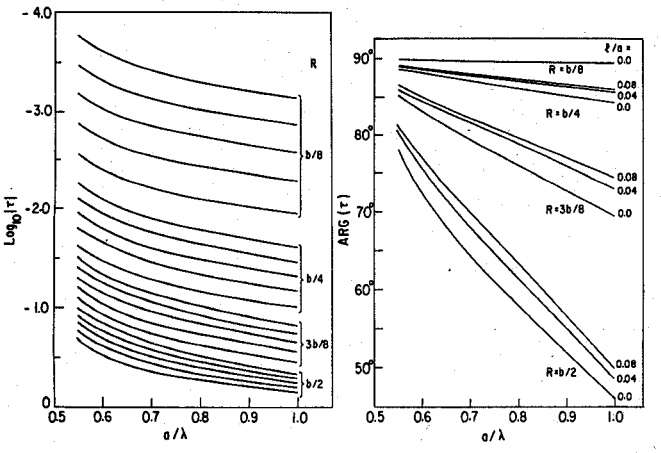

Fig. 7. Amplitude and phase of the transmission coefficient (TE_{10} mode) for a thick diaphragm, with centered circular hole, in rectangular waveguide. The thinnest diaphragm ($l = 0$) has the largest $|\tau|$.

aphragm thickness. Moreover, the effect is greater for small irises since in a guide of smaller radius the modes that try to "tunnel" across the diaphragm are more strongly attenuated.

The phase of the transmission coefficient, $\arg(\tau_{10})$, is plotted in Fig. 7(b). Here the thicknesses are $l/a = 0$, 0.04, and 0.08, except for the case of $R = b/8$, where the phase is almost invariant with thickness. The greatest phase change occurs for the largest hole ($R = b/2$). Not surprisingly, the phase is almost $+90°$ for small holes, since in such a case $\rho_{10} \simeq -1$ and (51b) must be satisfied.

VI. Discussion and Conclusions

This paper has provided an exact modal solution (in principle) to the problem of scattering at circular-to-rectangular waveguide junctions. In practice, numerical results for dominant-mode reflection and transmission coefficients accurate to 1 or 2 percent are possible when 12 modes are considered in the smaller circular guide. In the case of diaphragms with centered circular holes, the effect of the thickness of the diaphragm has been shown to be always significant (see Fig. 7). The effect of sidewall thickness in single and multiaperture waveguide couplers has previously been taken into account by Levy [13], who used the earlier small-aperture work of McDonald [14].

Although this paper has postulated throughout that the waveguides are perfectly conducting, the effect of a large but finite conductivity can be accommodated by a generalization of the conservation of complex power technique [15]. Moreover, the analysis of cavity resonators and filters formed by transverse diaphragms with centered circular holes is a quite simple extension of the present work, even if conductivity losses are included [15].

References

[1] H. A. Bethe, "Theory of diffraction by small holes," *Phys. Rev.*, vol. 66, pp. 163–182, Oct. 1944.
[2] N. Marcuvitz, Ed., *Waveguide Handbook*. New York: McGraw-Hill, 1951.
[3] A. Wexler, "Solution of waveguide discontinuities by modal analysis," *IEEE Trans. Microwave Theory Tech.*, vol. MTT-15, pp. 508–517, Sept. 1967.
[4] P. H. Masterman and P. J. B. Clarricoats, "Computer field-matching solution of waveguide transverse discontinuities," *Proc. Inst. Elec. Eng.*, vol. 118, pp. 51–63, Jan. 1971.
[5] R. E. Collin, *Field Theory of Guided Waves*. New York: McGraw-Hill, 1960, ch. 8.
[6] R. Vahldieck and J. Bornermann, "A modified mode-matching technique and its application to a class of quasi-planar transmission lines," *IEEE Trans. Microwave Theory Tech.*, vol. MTT-33, pp. 916–926, Oct. 1985.
[7] R. Mittra, T. Itoh, and T. S. Li, "Analytical and numerical studies of the relative convergence phenomenon arising in the solution of an integral equation by the moment method," *IEEE Trans. Microwave Theory Tech.*, vol. MTT-20, pp. 96–104, Feb. 1972.
[8] R. Mittra and S. W. Lee, *Analytical Techniques in the Theory of Guided Waves*. New York: Macmillan, 1971.
[9] R. Safavi-Naini and R. H. MacPhie, "Scattering at rectangular-to-rectangular waveguide junctions," *IEEE Trans. Microwave Theory Tech.*, vol. MTT-30, pp. 2060–2063, Nov. 1982.
[10] R. E. Collin, *Foundations for Microwave Engineering*. New York: McGraw-Hill, 1966, pp. 190–194.
[11] M. Abramowitz and I. A. Stegun, *Handbook of Mathematical Functions*. New York: Dover, 1965.
[12] R. R. Mansour and R. H. MacPhie, "Scattering at an N-furcated parallel-plate waveguide junction," *IEEE Trans. Microwave Theory Tech.*, vol. MTT-33, pp. 830–835, Sept. 1985.
[13] R. Levy, "Improved single and multiaperture waveguide coupling theory, including explanation of mutual interactions," *IEEE Trans. Microwave Theory Tech.*, vol. MTT-28, pp. 331–338, Apr. 1980.
[14] N. A. McDonald, "Electric and magnetic coupling through small apertures in shield walls of any thickness," *IEEE Trans. Microwave Theory Tech.*, vol. MTT-20, pp. 689–695, Oct. 1972.
[15] J. D. Wade, "The conservation of complex power technique and scattering from circular apertures in rectangular waveguides," M.A.Sc. thesis, University of Waterloo, Waterloo, Ontario, Canada, 1984.

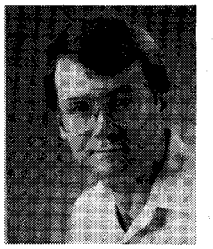

John Douglas Wade was born in London, Ontario, Canada, on March 27, 1953. He received the B.Sc. degree in physics from the University of Toronto in 1976, the M.Sc. degree in astronomy from the University of Western Ontario in 1979, and the M.A.Sc. degree in electrical engineering from the University of Waterloo, Ontario, in 1984.

He is presently with the National Research Council of Canada in Ottawa, where he is involved with the development of centimeter- and millimeter-wave receivers for the Algonquin Radio Observatory.

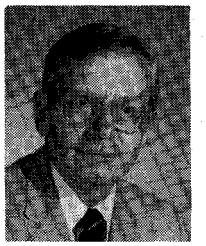

Robert H. MacPhie (S'57–M'63–SM'79) was born in Weston, Ontario, Canada, on September 20, 1934. He received the B.A.Sc. degree in electrical engineering from the University of Toronto in 1957 and the M.S. and Ph.D. degrees from the University of Illinois, Urbana, in 1959 and 1963, respectively.

In 1963, he joined the University of Waterloo, Waterloo, Ontario, Canada, as an Assistant Professor of electrical engineering and at present he is Professor of electrical engineering at Waterloo. His research interests currently focus on dipole antennas, waveguide scattering theory, scattering from prolate spheroid systems, and microstrip structures. During 1984–1985, he was on sabbatical leave as a Professeur Associé at the Université de Aix-Marseille I, France, working at the Département de Radioélectricité.